



Microstructure and Physical Characteristics of Novel Z-Type Hexaferrite with Cu Modification

HONGGUO ZHANG,^{1,*} JI ZHOU,² YONGLI WANG,² LONGTU LI,² ZHENXING YUE² & ZHILUN GUI²

¹Department of Materials Science, Laboratory for Electronic Materials and Devices, University of North Texas, Denton TX, 76203, USA

²State Key Laboratory of New Ceramics and Fine Processing, Department of Materials Science and Engineering, Tsinghua University, Beijing 100084, Peoples' Republic of China

Submitted January 15, 2002; Revised April 18, 2002; Accepted September 18, 2002

Abstract. The influence of Cu modification of physical characteristics of Co_2Z hexaferrites, which have stoichiometric compositions of $\text{Ba}_3\text{Co}_{2(1-x)}\text{Cu}_{2x}\text{Fe}_{24}\text{O}_{41}$ ($x \leq 0.50$), was investigated. The results show that the microstructure of modified hexaferrites is improved greatly. In the range of solid solubility of Cu, the cell parameters (a and c) of Co_2Z hexaferrites with Cu modification show a reverse change, a of hexagonal parameter decreases and c of axial parameter increases. The saturation magnetization, remnant magnetization, hysteresis behavior, initial permeability and quality factor as well as its possible affecting factors of Cu modified Co_2Z hexaferrites are also discussed in this paper.

Keywords: Z-type hexaferrite, Cu modification, cell parameters, magnetic characteristics

1. Introduction

There is an increasing interest in Co_2Z ferrite ($\text{Ba}_3\text{Co}_2\text{Fe}_{24}\text{O}_{41}$), which is considered an ideal candidate material for multi-layer chip inductors (MLCI), because Co_2Z ferrite has high performance in hyper-frequencies of 200–1000 MHz [1, 2]. Especially its high cut-off frequencies up to the 3 GHz region, compared with the 300 MHz ceiling encountered with the spinel ferrites, bring Co_2Z into the hyper-frequency region useful for chip inductors. Due to its special hexagonal structure, pure Co_2Z is very complicated and only formed at above 1300°C. However, for MLCI fabrication, it requires Co_2Z be sintered at a relatively low temperature of 850–900°C. How to drop the sintering temperature of Z-type ferrite becomes a key problem. Furthermore, the purity and stability of Z-type phase during sintering at low temperature is also a key problem.

From the crystallographic point of view, Co_2Z ferrite is among the most complex compounds in the family of hexaferrites with planar hexagonal structure.

The unit cell of a Co_2Z ferrite contains 140 atoms and belongs to the $\text{P6}_3/\text{mmc}$ space group. The hexagonal cell parameters a and c are 0.59 and 5.23 nm respectively [3]. The complexity of the structure mainly results from large Ba^{2+} . Since the radius of Ba^{2+} ion is comparable to the O^{2-} radius, it prefers the oxygen position rather than the interstitial site. Metal ions (Fe^{3+} , Fe^{2+} , Co^{2+} and Cu^{2+}), however, are located in non-equivalent interstitial sites. Theoretically, the Co_2Z ferrite, $\text{Ba}_3\text{Co}_2\text{Fe}_{24}\text{O}_{41}$, can be treated as a sum of two simple ferrites, namely M type ($\text{BaFe}_{12}\text{O}_{19}$) and Y type ($\text{Ba}_2\text{Co}_2\text{Fe}_{12}\text{O}_{22}$) ferrites. The extremely large elementary cell and the presence of “strongly anisotropic” Co^{2+} ion also lead to the complexity of its magnetic properties [4].

By now, there have been few literatures on low temperature sintering of Co_2Z reported. In this paper, Cu is incorporated into the pure $\text{Ba}_3\text{Co}_2\text{Fe}_{24}\text{O}_{41}$ as an effective constituent. Consequently, a compromise among various properties and low temperature sintering is expected to achieve. Furthermore, the possible micro mechanism involved in generating these changes in performance was discussed.

*To whom all correspondence should be addressed.

2. Experimental Procedure

2.1. Powder Synthesis and Sample Preparation

The stoichiometric composition of the $\text{Ba}_3\text{Co}_2(1-x)\text{-Cu}_{2x}\text{Fe}_{24}\text{O}_{41}$, where $0.00 \leq x \leq 0.50$, were prepared by the solid-state reaction method. The raw materials, BaCO_3 , Co_3O_4 , CuO and Fe_2O_3 , of AR grade ($\geq 99.5\%$), were mixed in a stainless steel ball mill under anhydrous ethanol for 4–6 hours. The mixed powders were first calcined at 1000–1050°C for 6 h in air. The calcined powders were ground and then pressed in a stainless-steel die under a pressure of about 40000–60000 N/m^2 with 5%wt PVA as lubricant. All pellet and toroidal samples were sintered at 1100–1150°C. Ag-Pd alloy was coated in both surfaces of the sintered pellets (10 mm diameter, 0.5–1.5 mm thickness) to measure the electrical properties. The toroidal samples (20 mm outside diameter, 10 mm inside diameter, about 3 mm thickness) were used to measure magnetic properties.

2.2. Microstructure Characterization

The phase structure of all samples were investigated by means of X-ray diffraction (XRD), using FeK_α radiation at 35 KV and 25 mA in the range of $2\theta = 35\text{--}70^\circ$

with a scanning speed of 0.5°/min. Scanning electron micrograph (SEM) was used to observe the microstructure of fracture surface of the sintered samples.

2.3. Property Characterization

The DC resistivity of the pellet samples was measured at room temperature with a HP4140A Meter. The dielectric constant, initial permeability and quality factor of toroidal samples were measured from 1–1000 MHz at room temperature by a HP4194A impedance analyzer. The other magnetic parameters of the corresponding $\text{Ba}_3\text{Co}_2(1-x)\text{Cu}_{2x}\text{Fe}_{24}\text{O}_{41}$ ferrite powders were detected by LDJ9600 VSM (Vibration Sample Magnetometer).

3. Results and Discussion

3.1. Phase Characterization and Variation of Cell Parameters

Figure 1 shows typical Z-type ($\text{Ba}_3\text{Co}_2\text{Fe}_{24}\text{O}_{41}$ planar hexagonal structure) of the sintered hexaferrites having $\text{Ba}_3\text{Co}_2(1-x)\text{Cu}_{2x}\text{Fe}_{24}\text{O}_{41}$ composition. However, with the increase of Cu content, a little traced Y phase ($\text{Ba}_2\text{Co}_2\text{Fe}_{12}\text{O}_{22}$ planar hexagonal structure) can be

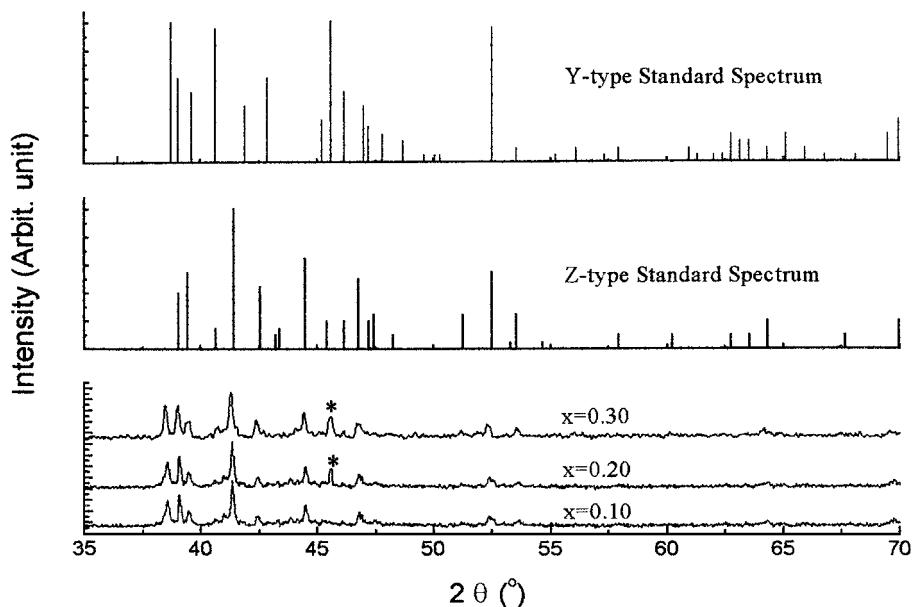


Fig. 1. XRD spectra of modified Co_2Z hexaferrites with different Cu contents, * means Y type phase.

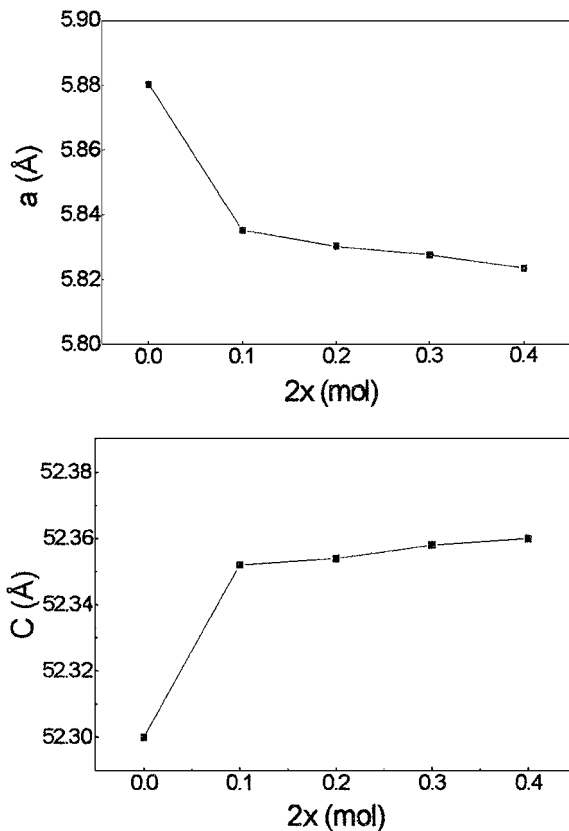


Fig. 2. Compositional variation of cell parameters (a and c) of Co_2Z hexaferrites with different Cu contents.

detected, and this is in accordance with Pullar's report [5]. The variation of cell parameters of samples with different Cu contents calculated using the crystallographic X-Ray Diffraction and Data Acquisition software accompanied by the Rigaku DMax A X-ray diffractometer is plotted in Fig. 2. It can be seen that, with the increase of Cu, the planar parameter of " a " gradually decreases whereas axial parameter of " c " increases. This mainly resulted from the different preference to the interstitials (A site: octahedral interstice; B site: tetrahedral interstice), which leads to the crystalline deformation and inner stress. When the inner stress of ferrites becomes saturated, the both parameters become stable [2].

3.2. Microstructure Characterization

Compared with pure $\text{Ba}_3\text{Co}_2\text{Fe}_{24}\text{O}_{41}$ [6], the compact and homogeneous microstructure of $\text{Ba}_3\text{Co}_{2(1-x)}\text{Cu}_{2x}\text{Fe}_{24}\text{O}_{41}$

can be observed at relatively low sintering temperatures, seen in Fig. 3. This should be attributed to the formation of a new solid solution $\text{Ba}_3\text{Co}_{2(1-x)}\text{Cu}_{2x}\text{Fe}_{24}\text{O}_{41}$, which has lower melting point than $\text{Ba}_3\text{Co}_2\text{Fe}_{24}\text{O}_{41}$ due to the incorporation of Cu. Meanwhile, the intergranular pores in $\text{Ba}_3\text{Co}_{2(1-x)}\text{Cu}_{2x}\text{Fe}_{24}\text{O}_{41}$ hexaferrites also greatly decrease. The 10–15 μm (length) of slim grain for $\text{Ba}_3\text{Co}_{2(1-x)}\text{Cu}_{2x}\text{Fe}_{24}\text{O}_{41}$ is much smaller than 20 μm of platelet grain sizes of $\text{Ba}_3\text{Co}_2\text{Fe}_{24}\text{O}_{41}$. This indicates that grain growth is sufficiently suppressed by the Cu incorporation and preference position, because the low temperature sintering can only lead to small grain size in all directions. Furthermore, since the melting point of CuO is 1026°C, appropriate segregation and volatilization of Cu may occur, which not only improves grain morphology and distribution of inner pores [7], but also inhibits the generation of Fe^{2+} (Fe^{2+} was not detected by wet chemical analysis), this also implies that the Cu content x is possibly nominal in our paper.

Due to the incorporation of Cu^{2+} , the relative changes of magnetocrystalline anisotropy in Z-type hexaferrite occur due to different preference to interstitials of metal ions [2]. This can be not only observed from the variation of magnetic parameters (saturation magnetization, coercive force and remnant magnetization et al.) of the corresponding $\text{Ba}_3\text{Co}_{2(1-x)}\text{Cu}_{2x}\text{Fe}_{24}\text{O}_{41}$ ferrites listed in Table 1, but also implied from the variation of cell parameters and grain growth mainly proceeding in a three-dimensional manner. As to the process of atom transportation and variation of crystalline structure (from single oxide, spinel to M, Y and finally Z type hexaferrites) it has not been known well by far [3].

3.3. Properties Characterization

Figure 4 shows the frequency dependence of the initial permeability and quality factor for Cu modified samples. Although the initial permeability of about 9–10.3 is a little bit lower than 11.5 of pure Co_2Z , the quality factor of modified hexaferrites is much higher than that of pure Co_2Z , especially in hyper frequency of 100–800 MHz [6]. It also can be observed that it is in basic accordance with Snoek law [8]. Just like spinel ferrite, the magnetism of hexaferrites mainly results from the combination of spin rotation and domain wall motion, and is determined by the grain size, densification, saturation magnetization, and internal stress

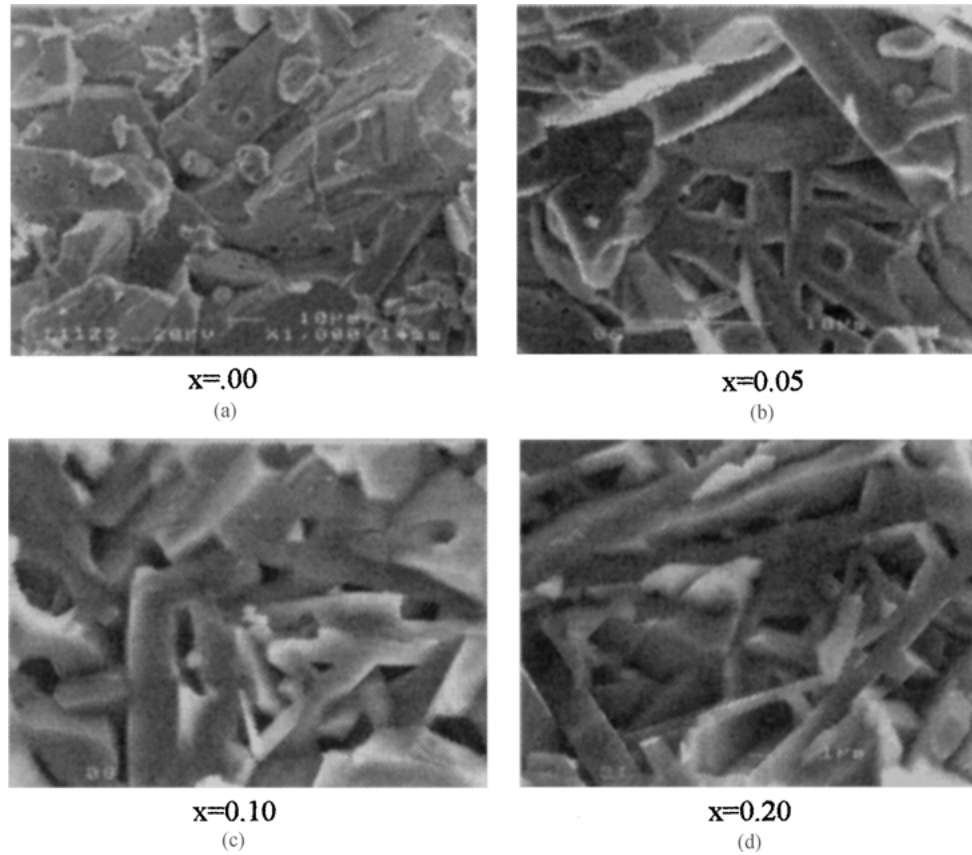


Fig. 3. SEM micrographs of the different samples sintered at different temperatures for 4 hours: (a) $x = 0.00$, 1270°C; (b) $x = 0.05$, 1180°C; (c) $x = 0.10$, 1125°C and (d) $x = 0.20$, 1100°C.

et al. However, suppressed grain growth, which commonly takes place in polycrystalline isotropic ferrites, should be the main reason for the decrease of initial permeability.

Z-type hexaferrite is one of the most complex compounds in the family of ferrites. The complexity mainly results from large Ba^{2+} . Since the radius of Ba^{2+} is comparable to the O^{2-} radius, Ba ions prefer the

Table 1. Compositional variation of key magnetic characteristic parameters, densities, DC resistivity, dielectric constant in $\text{Ba}_3\text{Co}_2(1-x)\text{Cu}_x\text{Fe}_{24}\text{O}_{41}$ system.^a

x	D (X-ray) (g/cm^3)	D (sintered) (± 0.05) (g/cm^3)	Ion moment (μ_B)				σ_s (± 1.0) (emu/g)	σ_r (± 0.5) (emu/g)	H_c ($\pm 5 \text{ O}_e$)	T_c ($\pm 5 \text{ K}$)	ρ ($\times 10^7 \Omega\text{cm}$) (25°C)	ε (± 0.5) (at 400 MHz)
			Fe^{3+}	Fe^{2+}	Co^{2+}	Cu^{2+}						
$x = 0.00^b$	5.31	4.54	5	4	2	1	68.34	2.66	25.28	670	2.61	39
$x = 0.10$	5.31	4.59	5	4	2	1	52.14	4.63	45.28	610	3.42	23
$x = 0.20$	5.31	4.65					50.82	9.79	110.89	575	3.71	21
$x = 0.30$	5.31	4.71					49.59	8.90	111.73	530	3.77	21
$x = 0.40$	5.31	4.73					48.11	7.65	140.86	505	3.67	19

^a D -density; σ_s -saturation magnetization; σ_r -remnant magnetization; H_c -coercive force; T_c -Curie temperature; ρ -DC resistivity; ε -dielectric constant.

^b $x = 0.00$, pure Co_2Z , sintered at 1290°C/4 h.

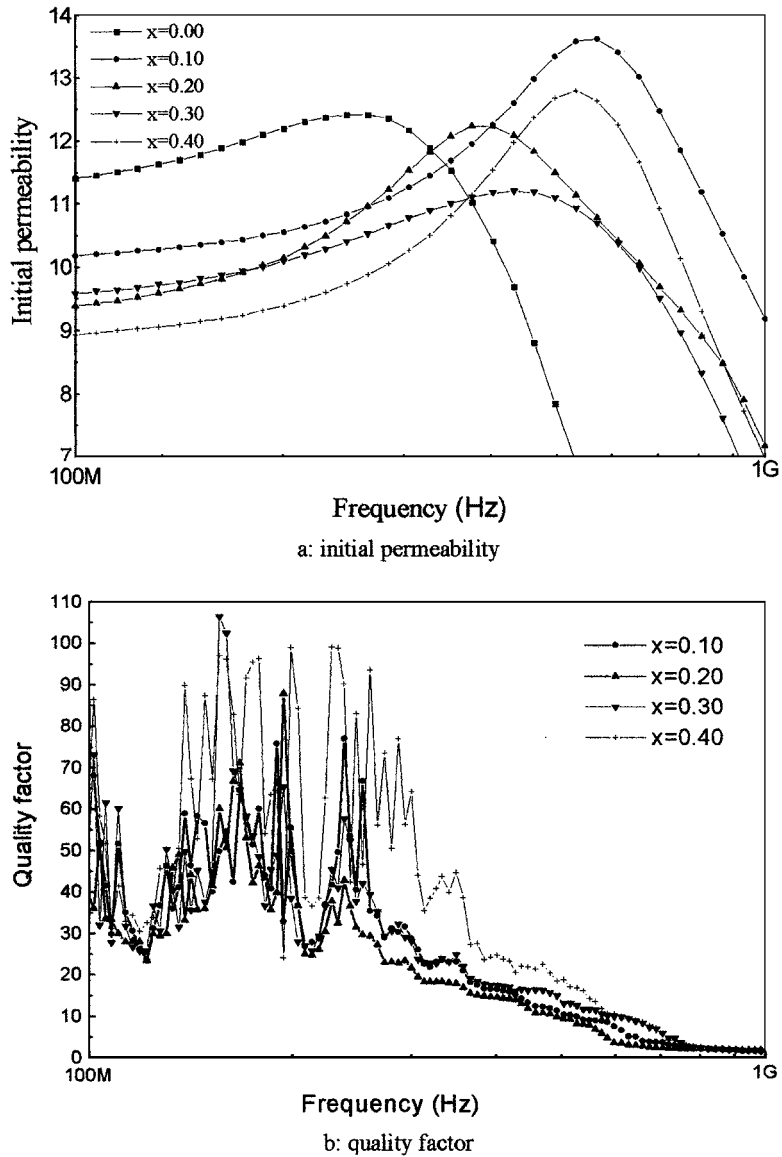


Fig. 4. Frequency dependence of initial permeability and quality factor for the modified samples.

oxygen positions to the interstitial sites. Metal ions (Fe^{3+} , Co^{2+} and Cu^{2+}), however, are located in non-equivalent interstitial sites and, Co^{2+} belongs to the strongly magnetocrystalline anisotropic element. All these can lead to the complexity of its magnetic properties [4].

When Cu^{2+} enters the lattice interstitial, strong Fe-Fe interactions that dominate in saturation magnetization are partially replaced by weak Cu-Fe interactions, indicated in Table 1. This weak ferro-

magnetic interaction degrades saturation magnetization. Moreover, Cu^{2+} prefers B site and this will modify the distribution of the Fe^{3+} ions on the two sublattices (A site: octahedral interstice; B site; tetrahedral interstice). As is known, the hexagonal ferrite consists of basic spinel blocks with certain alignments [2], due to its electronic configuration, ion radius difference and different electron affinity, Cu^{2+} will change the distribution of Co and Fe ions, and thus distort the lattice or crystalline field, and then generate an

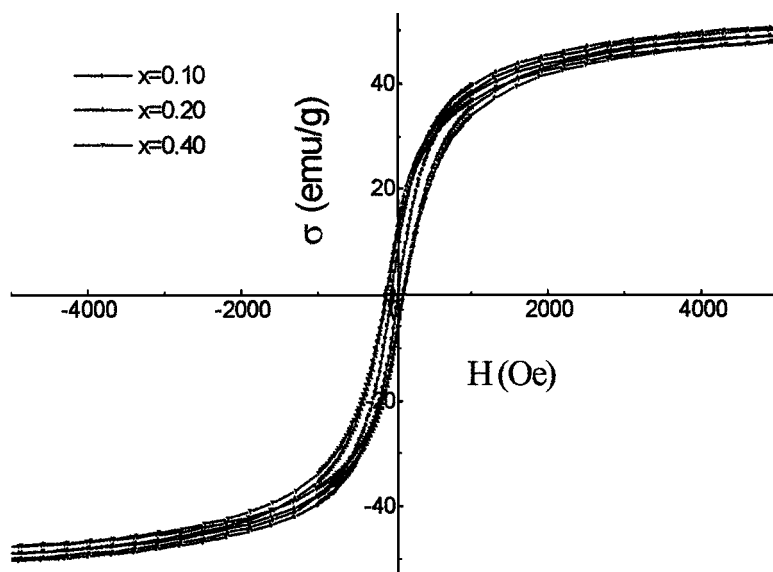


Fig. 5. Hysteresis behavior of the Cu-modified hexaferrite samples.

internal stress that will hinder the domain wall motion or spin rotation, this is just like the Ni-Zn-Cu spinel ferrites. Consequently, the permeability decreases [9, 10].

The variation of Curie temperature (T_c) for the samples is listed in Table 1. It can be seen that T_c decreases for the $\text{Ba}_3\text{Co}_2(1-x)\text{Cu}_{2x}\text{Fe}_{24}\text{O}_{41}$ with the increase of Cu. As stated in references 1 and 2, T_c is determined by the strong magnetic interaction among various ions. So, the decrease of number of Fe-Fe or Co-Fe strong magnetic interaction results in the reduction of T_c according to Smit's report [1, 2].

Figure 5 shows the hysteresis behavior of Cu modified hexagonal ferrites. It can be seen that the areas of the hysteresis curves of three samples are all very small. This indicates that the typical soft magnetic crystalline phase exists in the samples, when low melting point Cu was incorporated, no hard magnetic phase occurred, this will be beneficial for future application in the MLCI production.

The DC resistivity is more than $3.40 \times 10^7 \Omega\text{cm}$ and, dielectric constant is measured to be about 20 at 400 MHz, seen in Table 1. However, the resistivity values are essential for the bulk and the electrode resistance is negligible [11]. As to the variation of DC resistivity and dielectric constant, it is mainly correlated to the hopping probability of Fe^{3+} and the opportunity of Fe^{2+} formation [12]. The de-

tailed investigation will be reported in the forthcoming paper.

4. Conclusions

The proper incorporation of Cu with low melting point into $\text{Ba}_3\text{Co}_2\text{Fe}_{24}\text{O}_{41}$ can form typical Z-type hexagonal phase at relatively low sintering temperatures, not only improve densification and microstructure by the formation of compounds with low melting points, but also obtain excellent compromise magnetic properties: average 9.5 of initial permeability, over 20 of quality factor and about 1 GHz of cut-off frequency, compared with the pure Co_2Z hexaferrites. Due to the formation of Z-type hexaferrites at temperature ranging from 1050 to 1130°C, it is expected to have great potentiality to meet requirements for low temperature sintering of MLCI.

Acknowledgments

The authors are indebted to the financial support from DARPA of USA (Grant: DAAD16-00-C-9273 and DARPA/SPAWAR N66001-00-1-8928, Chinese "863" High-Tech Project (Grant 2001AA325020), Chinese National Natural Science Foundation (Grant: 59995523), and the Ceramic Technology Center,

Motorola Inc., U.S.A. We would like to thank Dr. Huang for his beneficial discussion about XRD and properties measurements.

References

1. J.H. Jonker, H.P.J. Wijn, and P.B. Braun, *Philips Tech. Rev.*, **18**, 145 (1957).
2. J. Smit and H.P. Jones, *Ferrites, Physical Properties of Ferromagnetic Oxides in Relation to their Applications* (Philips Technical Library, Eindhoven, 1959).
3. S. Nicolopoulos, M. Vallet-Regi, and J.M. Gonzalez-Calbet, *Mater. Res. Bull.*, **25**, 567 (1990).
4. J.H. Hankiewicz, *J. Magn. Magn and Mater.*, **101**, 134 (1991).
5. R.C. Pullar, S.G. Appleton, and A.K. Bhattacharya, *J. Magn. Magn. Mater.*, **186**, 313 (1998).
6. H.G. Zhang, Ji Zhou, and Z.L. Gui, *Mater. Sci. Eng.*, **B65**, 184 (1999).
7. J.E. Burke and W.D. Kingery (Ed.), *Ceramic Fabrication Processes* Vol. 120 (Wiley, New York, 1958).
8. J.L. Snoek, *Nature*, **160**, 90 (1947).
9. T. Nakamura, *J. Magn. Magn and Mater.*, **168**, 285 (1997).
10. C.S. Kim, W.C. Kim, S.Y. An, and S.W. Lee, *J. Magn. Magn and Mater.*, **215**, 213 (2000).
11. H.G. Zhang, Y. Wang, and L.L. Li, *J. Jpn. Ceram. Soc.*, **109**(7), 587 (2001).
12. P. Allegri, D. Autissier, and T. Taffary, *Key Eng. Mater.*, **132-136**, 1424 (1997).